TECHNICAL MEMORANDUM

775

How rare is the Draupner wave event?

Peter A.E.M. Janssen

Research Department

December 2015

This paper has not been published and should be regarded as an Internal Report from ECMWF.
Permission to quote from it should be obtained from the ECMWF.

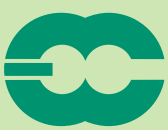

European Centre for Medium-Range Weather Forecasts
Europäisches Zentrum für mittelfristige Wettervorhersage
Centre européen pour les prévisions météorologiques à moyen terme

Series: ECMWF Technical Memoranda

A full list of ECMWF Publications can be found on our web site under:
http://www.ecmwf.int/en/research/publications

Contact: library@ecmwf.int

©Copyright 2015

European Centre for Medium-Range Weather Forecasts
Shinfield Park, Reading, RG2 9AX, England

Literary and scientific copyrights belong to ECMWF and are reserved in all countries. This publication is not to be reprinted or translated in whole or in part without the written permission of the Director-General. Appropriate non-commercial use will normally be granted under the condition that reference is made to ECMWF.

The information within this publication is given in good faith and considered to be true, but ECMWF accepts no liability for error, omission and for loss or damage arising from its use.

Abstract

Cavaleri *et al.* (2015) have produced a simulation of the famous Draupner wave event (that occurred on the 1^{rst} of January 1995 at 15:20 at the Draupner platform) using a new, high-resolution version of the ECMWF forecasting system. According to this simulation, which has a horizontal resolution of about 10 km and 137 layers in the vertical, there are clear signs that around the time of the wave event evidence of the presence of a polar low is found resulting in a sea state consisting of two systems, namely a windsea and a swell. As suggested by a study of M. Onorato such two-component systems might be more prone to Modulational Instability giving rise to higher probabilities of extreme events, but the two systems need both to be narrow band.

After providing an overview of the theoretical probablistic approach that will be followed (which includes new results on how to determine skewness and envelope kurtosis for general spectra), the extreme statistics over the first 20 hours of the forecast at the Draupner platform are presented. It is found that there is some evidence to suggest that at the time of the freak wave event the statistics in terms of 'envelope' skewness and kurtosis are exceptional. In addition, one might ask the question how likely the occurrence of this freak wave event is. Then, for a domain of 10×10 km^2, which corresponds to the spatial resolution of the wave model used in the simulation, it is found that the probability that maximum wave height is equal or larger than the maximum Draupner wave height is about 13%. This is a fairly large probability, but it should be noted that in order to achieve these large probabilities, one needs to introduce a number of nonlinear effects, related to skewness and kurtosis, in the probability distribution function (pdf) of wave height. Using Gaussian statistics, corresponding to linear waves, the probability drops to only 0.5%, hence, according to linear theory, the Draupner wave event is not very likely.

Finally, by comparing with results from the T_l 799 (about 25 km) version of the ERA-interim software it is clear that for a realistic simulation of this extreme event spatial resolution matters. The new version of the ECMWF model allows the simulation of a small-scale polar low which is absent in the ERA-interim run. As a consequence, the sea state in the high-resolution run is much steeper and contains longer waves so that near the Draupner location with depth of 69 m shallow water effects are much more important, giving an enhancement of probabilities at the time the Draupner event occurred. On the other hand, the ERA-interim simulation, which has shorter, less steep waves, does not suggest that the sea state has extreme statistics.

1 Introduction.

In this note I report on my findings regarding how likely the occurrence of the Draupner freak wave event is in the light of present day understanding of the dynamics of ocean waves.

In §2 a description of the method is given. Starting point for this is Janssen (2014) which describes an analysis of time series based on the envelope ρ. The square of the envelope is a measure for the potential energy of the waves, E. In fact, one has $E = \rho^2/2$ and this is a popular measure to characterize extreme events in fields such as nonlinear optics because only the envelope of the wave train can be observed but not the wave train itself. I suggest to use the same measure in the field of ocean waves as it is a measure that has physical relevance. For convenience, and to stay close to oceanographic practice, I will also use the envelope wave height h which is defined to be twice the envelope height, i.e. $h = 2\rho$. If the effects of nonlinearity are small, the pdf of envelope wave height may be obtained by means of a Taylor expansion of the logarithm of its generating function. This basically gives an expansion where the coefficients are the third-order (skewness) and fourth-order (kurtosis) cumulants of the random envelope. Here, envelope skewness and kurtosis for the bound waves can in principle be obtained from the wave spectrum following a procedure in Janssen (2009), who applied it to obtain the surface elevation statistics, while the contribution from the free waves is obtained from Janssen (2003). This approach seems to work well as follows from comparisons with pdf's observed in the laboratory.

Nevertheless, this statistical theory has a restricted range of validity. From a comparison with maximum wave height data obtained in the field by Janssen and Bidlot (2009) (see their Fig. 8) it is evident that the theoretical pdf starts to deviate from the observed one for extreme sea states with $h_{max}/H_S > 2.5$. Since for the Draupner wave event the envelope wave height is about three times the significant wave height it follows that this event is clearly outside the domain of validity of the present theory and an extension of the validity range is required.

Nowadays there is ample evidence that for very extreme (sea) states the pdf of envelope wave height has an exponential tail, resulting, compared to the present theory, in much larger probabilities for extreme events. Evidence for an exponential tail follows from numerical simulations (e.g. Janssen (2014) and the Appendix), comparison with field data (Janssen and Bidlot, 2009), but the range over which the exponential tail is found is fairly small. The reason for this fairly small range is related to the fact that in oceanography we are dealing with a limited amount of extreme events. On the other hand, in nonlinear optics and liquid crystals the amount of extreme events is much larger so that accurate estimates may be given for even small probabilities, of the order of 10^{-6} and even smaller. As a consequence, the tail of the pdf may be observed over a much wider range and the experimental evidence suggest that this tail is exponential. It is therefore important to modify the present approach by adding an exponential tail. For liquid crystals, S. Residori mentioned to me (Residori, private communication, 2015; Montina *et al.*, 2009) that the probability distribution function $p(E)$, with E the power of the signal normalized with its average, can be approximated by the following simple empirical form,

$$p(E) = Ne^{-\sqrt{c_1+c_2E}},$$

where the normalization factor N and the coefficients c_1 and c_2 follow from a fit with the observations. This is a very intriguing form as it describes a gradual transition from a Gaussian state to a state determined by an exponential distribution. Rather than fitting to observations, the relevant parameters will be determined by matching with the approximate expression of the wave height probability at the edge of its range of validity. Thus, the fitting parameters will implicitely depend on the value of skewness and kurtosis obtained from the two-dimensional spectrum.

In §2 and §3 I will describe and discuss the application of this modified method to the Draupner case. I will concentrate on the question how likely the Draupner freak wave event is in the context of the present formalisme. I will do this using the maximum wave height distribution. It is remarked that normally one determines the maximum wave height distribution for a time series of 20 min. length. Thus, one typically deals with a few hundred events. Here I suggest a somewhat different approach, which is based on the assumption that extreme events are caused by constructive interference, and since the waves are of finite amplitude the sea state has finite skewness and kurtosis which will give rise to an additional amplification of the extreme event. In addition, when the sea state is sufficiently coherent the Benjamin-Feir instability (Benjamin and Feir, 1967) will give rise to an additional focussing of wave energy during the extreme event. In other words, an extreme event is similar to the luck of the draw from the lottery, since we have no detailed knowledge of the phases of the individual waves. For this reason a statistical approach seems to be appropriate, but clearly this approach cannot be validated directly against exceptional, singular events such as the Draupner case. At best one should be able to determine how likely such an event is in the context of our model of 'reality'. I decided therefore to determine for a domain of the size of the model grid box the probability that maximum wave height exceeds or is equal to the observed value at the Draupner location. Evaluation of this exceedance probability relies, of course, on an accurate modelling of the tail of the distribution, while it is also sensitive to the estimation of the number of events in a spatial domain.

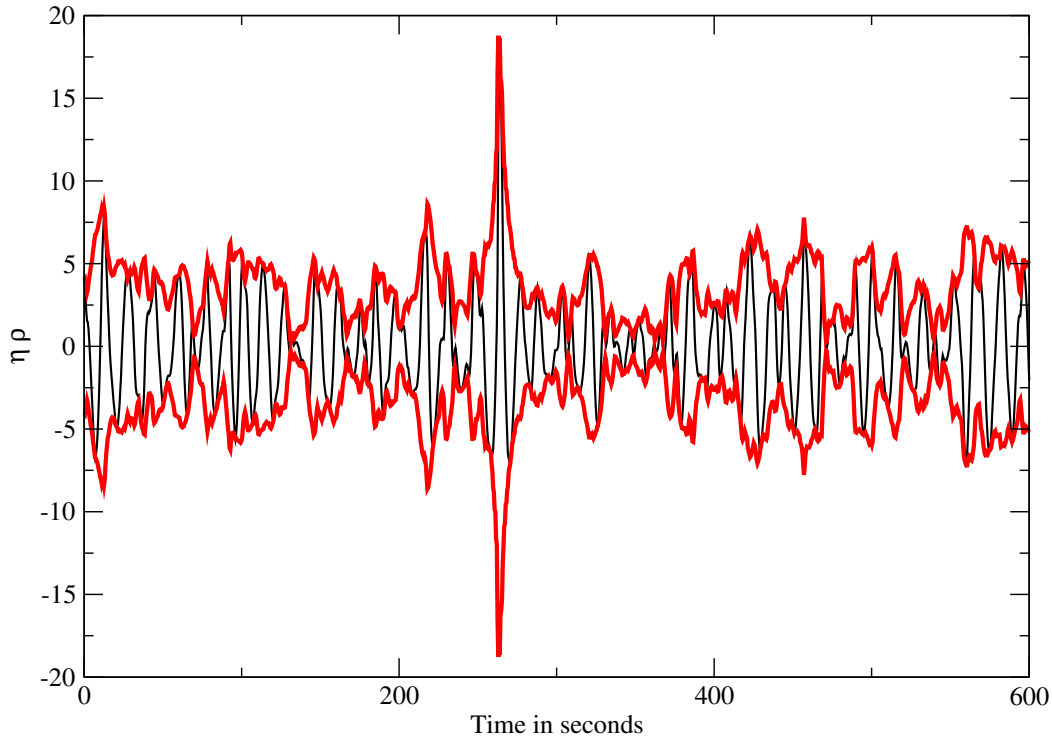

Figure 1: Time series η of the Draupner freak wave (black). The envelope time series ρ is shown in red and it clearly shows how extreme this event is. The corresponding local wave energy at the maximum is about 20 times the average wave energy.

2 The method.

Following Janssen (2014) a time series analysis based on the envelope wave height will be used. In Fig. 1 I show the timeseries of surface elevation and envelope, where the envelope was obtained by Miguel Onorato using the Hilbert transform. The figure clearly shows that extreme events are well characterized by the envelope method. To make things more quantitative let us introduce the local energy $\mathscr{E} = \langle \eta^2 \rangle$ and introduce the envelope ρ according to $\eta = \rho \cos\theta$. One finds

$$\mathscr{E} = \frac{1}{2}\rho^2, \tag{1}$$

while the normalized local energy is given by $E = \mathscr{E}/\sigma^2$ with $\sigma^2 = m_0$ the variance of the sea surface and m_0 the zeroth moment of the spectrum. The value $E = 1$ then corresponds to a local wave energy which equals the average wave energy in the domain of interest. The Draupner wave event has $E \simeq 20$ which illustrates that at the focal point there has been a considerable amplication of wave energy, therefore this is quite an extreme event. As an alternative measure I introduce the local wave height as twice the envelope height ρ and the normalized envelope wave height h becomes

$$h = \frac{2\rho}{4\sigma} \tag{2}$$

and the relation between normalized envelope wave height and local energy is $E = 2h^2$ so that for the Draupner event $h_{max} = 3.1$.

Janssen (2014) has obtained the following envelope wave height distribution for a weakly nonlinear sea state. It reads

$$p(h) = 4he^{-2h^2}\left\{1 + C_4\left(2h^4 - 4h^2 + 1\right) + C_3^2\left(4h^6 - 18h^4 + 18h^2 - 3\right)\right\}. \tag{3}$$

where the parameters C_4 and C_3^2 follow from knowledge of the two-dimensional wave spectrum and are related to the kurtosis and skewness of the sea state. The envelope kurtosis κ_4 is given by

$$\kappa_4 = \kappa_{40} + 2\kappa_{22} + \kappa_{04} \tag{4}$$

so that

$$C_4 = \frac{\kappa_4}{8}, \tag{5}$$

while

$$C_3^2 = \frac{\kappa_3^2}{72},\ \kappa_3^2 = 5(k_{30}^2 + \kappa_{03}^2) + 9(\kappa_{21}^2 + \kappa_{12}^2) + 6(\kappa_{30}\kappa_{12} + \kappa_{03}\kappa_{21}) \tag{6}$$

The κ's refer to a number of cumulants of the joint distribution of the surface elevation η and its Hilbert transform ζ. In addition, it is noted that both free and bound waves may contribute to the cumulants.

From the pdf for wave height, Eq. (3), one may then immediately obtain the pdf of wave energy, since $p(h)\mathrm{d}h = p(E)\mathrm{d}E$ with $E = 2h^2$. The result is

$$p(E) = e^{-E}\left[1 + C_4 A(E) + C_3^2 B(E)\right], \tag{7}$$

where

$$A(E) = \frac{1}{2}E^2 - 2E + 1,\ B(E) = \frac{1}{2}E^3 - \frac{9}{2}E^2 + 9E - 3. \tag{8}$$

Finally, for the purpose of estimating the maximum wave height distribution the exceedance probability $P(E > E_c)$ is required. It follows from an integration of the pdf (7) from E to infinity, with the result

$$P(E) = e^{-E}\left[1 + C_4 A(E) + C_3^2 B(E)\right], \tag{9}$$

where

$$A(E) = \frac{1}{2}E(E-2),\ B(E) = \frac{1}{2}E(E^2 - 6E + 6). \tag{10}$$

2.1 Free waves.

The free wave case has been discussed extensively by Mori and Janssen (2006). For the free waves the skewness vanishes while the kurtosis enjoys certain symmetry properties in such a way that $\kappa_{04} = \kappa_{40}$ while $\kappa_{22} = \kappa_{40}/3$ so that

$$C_4^{free} = \frac{1}{3}\kappa_{40}^{dyn}, \tag{11}$$

where κ_{40}^{dyn} is explicitely given by Janssen (2003) in terms of the directional angular frequency spectrum $E(\omega,\theta)$, i.e.

$$\kappa_{40}^{dyn} = \frac{12g}{m_0^2}\int \mathrm{d}\theta_{1,2,3}\mathrm{d}\omega_{1,2,3}T_{1,2,3,4}\sqrt{\frac{\omega_4}{\omega_1\omega_2\omega_3}} \times R(\Delta\omega,t)E_1E_2E_3. \tag{12}$$

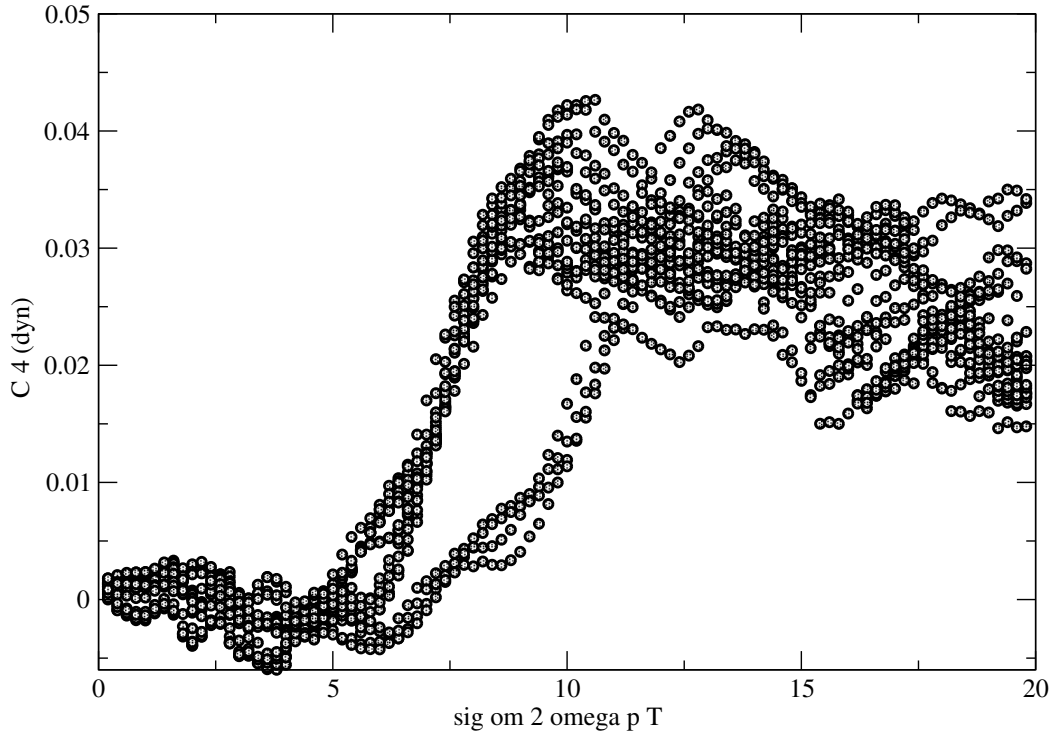

Figure 2: Evolution of dynamic kurtosis $\kappa_{40}^{dyn}/3$ as function of the dimensionless time $\tau = \sigma_\omega^2 \omega_p T$, where σ_ω is the relative width of the frequency spectrum and ω_p is the peak wavenumber.

Here, the time-dependent real part of the resonance function $R(\Delta\omega,t) = [1-\cos(\Delta\omega t)]/\Delta\omega$, the frequency mismatch $\Delta\omega = \omega_1 + \omega_2 - \omega_3 - \omega_4$, while the fourth wave number follows from the resonance condition in wave number space, i.e. $\mathbf{k}_4 = \mathbf{k}_1 + \mathbf{k}_2 - \mathbf{k}_3$. The frequency ω_4 is obtained by evaluating the dispersion relation at the fourth wavenumber. Eq. (12) gives the evolution in time of the dynamic part of the kurtosis for given wave spectrum. In general no solution is known so a numerical evaluation of this six-dimensional integral is required. I have written software to calculate κ_{40}^{dyn} for arbitrary spectra and arbitrary depth such that $k_p D > 0.7$. The software has been validated for a number of special cases of which the solution is known, namely for Gaussian spectra in the narrow-band approximation. It should be realized that Eq. (12) is quite expensive to evaluate because it involves a six-dimensional integral. With a resolution of 36 frequencies and directions we are looking at $36^6 = 2,18$ Billion evaluations of the transfer coefficient which is quite substantial. For this reason I inspected before hand the simulated spectra of the Draupner case as provided by L. Bertotti. It turns out that a large part of the frequency-direction space contained small values so that I filtered the evaluation of the integrals accordingly. This filtering operation reduced the number of evaluations of the transfer coefficient to about 11 million. The time evolution of the dynamic kurtosis of all the 21 spectra is shown in Fig. 2, where time is scaled with the parameter $\sigma_\omega^2 \omega_p$ with σ_ω the relative frequency width and ω_p the peak frequency. The time scale $\tau_{nl} = 1/\sigma_\omega^2 \omega_p$ is the natural time scale that occurs when one assumes that the wave spectrum is narrow-band so that the evolution of the waves is determined by the nonlinear Schrödinger equation. Fig. 2 shows a surprisingly universal behaviour of the time evolution of the kurtosis, having an overshoot followed by a leveling off. The saturation occurs on a fairly long time scale of a few hundred wave periods and for estimating the severeness of the sea state the mean value of kurtosis averaged over the second half of the period will be used.

2.2 Bound waves.

As shown in Janssen (2014) the properties of the statistics of the bound waves is different from that of the free waves. Regarding the skewness I have now shown that for general spectra the following result is found:

$$\kappa_{12} = \frac{\kappa_{30}}{3}, \kappa_{21} = \kappa_{03} = 0, \tag{13}$$

where κ_{30} follows from knowledge of the wave spectrum, i.e.

$$\kappa_{30} = \frac{3}{m_0^{3/2}} \int \mathrm{d}\mathbf{k}_{1,2} E_1 E_2 \left(\mathscr{A}_{1,2} + \mathscr{B}_{1,2} \right), \tag{14}$$

where the coupling coefficients are given in Janssen (2009). As a consequence one finds for the skewness factor given in Eq. (6),

$$C_3^{bound} = \frac{\kappa_{30}}{3}. \tag{15}$$

A similar analysis can be performed to obtain a general expression for the envelope kurtosis. This is a very laborious task, however, and to make sure of the result I have taken the narrow-band limit which is in perfect agreement with an expression for the envelope kurtosis for a single nonlinear wave train. Finally, the single mode expression has been validated against numerical simulation of the Stokes wave train. Some of the details are given in the Appendix. For general spectra one finds for the envelope kurtosis κ_4 the result

$$\kappa_4 = \frac{32}{m_0^2} \int \mathrm{d}\mathbf{k}_{1,2,3} E_1 E_2 E_3 \left\{ \mathscr{A}_{1,2}\mathscr{A}_{2,3} + \mathscr{A}_{1,2}\mathscr{B}_{2,3} + \frac{1}{2}\mathscr{C}_{1+2-3,1,2,3} H_{1+2-3} \right. \\ \left. + \mathscr{B}_{1,3}\mathscr{B}_{3,2} \left[H_{3-2}H_{3-1} + H_{2-3}H_{1-3} \right] \right\} \tag{16}$$

where, again, the coupling coefficients are given in Janssen (2009). Then, the bound-wave part of the kurtosis factor C_4 follows from (5), hence,

$$C_4^{bound} = \kappa_4/8. \tag{17}$$

The contributions by the bound waves to skewness and kurtosis have been evaluated as well, and in Fig. 3 are shown the contributions of both free and bound waves to the kurtosis factor C_4 and the bound waves contribution to C_3 for all the 21 simulated spectra. There is an indication that around the time of the freak wave event the sea state was more extreme, this is seen in particular for the skewness factor which has a maximum at 16.00 hrs, and even more pronounced for the kurtosis factor. In order to try to understand the increase in stats around the Draupner event, the Appendix shows for the single mode result a plot of the depth dependence of the skewness C_3 and kurtosis factor C_4. For a dimensionless depth $x = k_0 \times h$ less then 2, the kurtosis factor is seen to increase quite rapidly. Therefore, because of this sensitive dependence on depth, it is of vital importance to have a realistic simulation of the sea state, in particular regarding aspects such as the steepness of the waves and their peak wavelength.

2.3 Adding an exponential tail.

Nowadays there is ample evidence that for very extreme (sea) states the pdf of envelope wave height has an exponential tail, resulting, compared to the present theory, in much larger probabilities for extreme

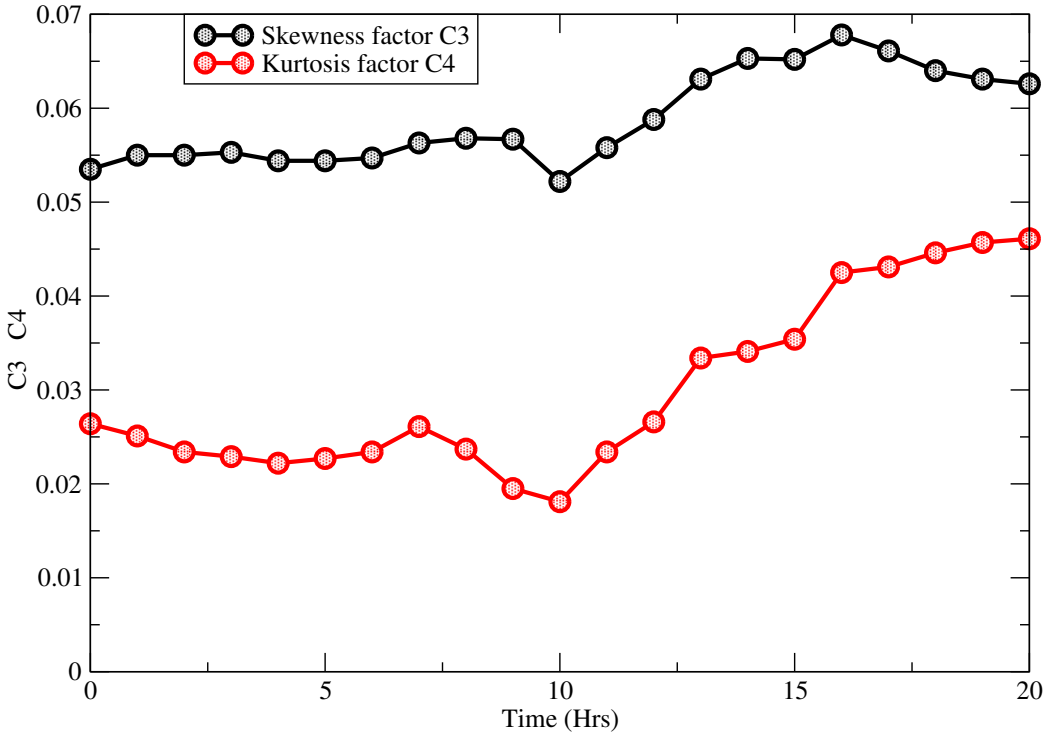

Figure 3: Evolution in time of simulated skewness and kurtosis factors C_3 and C_4 on the 1^{rst} of January 1995 at the Draupner platform.

events. Evidence for an exponential tail follows from numerical simulations (e.g. Montina *et al.* (2009), Walczak *et al.* (2015), Janssen (2014), see also the Appendix), and comparison with field data (Janssen and Bidlot, 2009). Also, in nonlinear optics and liquid crystals a considerable amount of experimental evidence is available that suggests that this tail is exponential. It is therefore important to modify the present approach by adding an exponential tail. For extreme waves in a nonlinear optical cavity Montina *et al.* (2009) have noted that the observed probability distribution function for intensity E can be well approximated by the following simple stretched exponential form

$$p(E) = Ne^{-\sqrt{c_1+c_2E}}$$

where $1/c_1$ provides a measure for deviations from Gaussian statistics which gives an exponential distribution. This empirical form has still three unknowns, namely a normalization factor N and the coefficients c_1 and c_2. After some trial and error it was realized that by using a stretched exponential to approximate the cumulative distribution function (CDF) only two fitting coefficients were needed.[1] I therefore decided to match the form

$$P(E) = \int_E^\infty \mathrm{d}x\, p(x) = e^{-z},\ z = -\alpha + \sqrt{\alpha^2 + \beta E}, \tag{18}$$

to the theoretical CDF (10) for normalized wave energy E. In order to do so one only needs to determine the parameters α and β.

[1] One could equally well fit the stretched exponential form (18) to the theoretical pdf. I have performed this exercize, but it was found that the relative rms error of the fit was typically twice as large compared to fitting the stretched exponential to the CDF, i.e. 11% versus 4.5%.

This simple form has some interesting properties. First of all, the condition $P(E) = 0$ is automatically satisfied so that the underlying pdf $p(E)$ is normalized to 1. Second, for small E Taylor expansion of z gives $z = \beta E/(2\alpha)$ hence

$$\lim_{E\to 0} P(E) = e^{-\frac{\beta}{2\alpha}E}, \tag{19}$$

while for large E one finds

$$\lim_{E\to\infty} P(E) = e^{-\sqrt{\beta E}}. \tag{20}$$

Realizing that $E = 2h^2$ this means that according to (19) for small E we have a Gaussian distribution while according to (20) for large E there is an exponential distribution.

By differentiation of the CDF (18) it is straightforward to obtain the pdf $p(E)$. By definition

$$p(E) = -\partial P/\partial E$$

so that

$$p(E) = \frac{\beta}{2(z+\alpha)} e^{-z},\ z = -\alpha + \sqrt{\alpha^2 + \beta E}. \tag{21}$$

The moments of the probability distribution function are defined as

$$I_n = \langle E^n \rangle = \int \mathrm{d}E E^n p(E),\ n = 1,2,3,.... \tag{22}$$

Partial integration and utilizing that the CDF has a simple exponential form the moments may be written as an integral over the CDF P, or

$$I_n = \int \mathrm{d}z E^n P(z),\ n = 1,2,3,..., \tag{23}$$

and E can be expressed in terms of z, $E = (z^2 + 2\alpha z)/\beta$. It is then possible to obtain expressions for the moments. The first few are

$$I_0 = 1, \tag{24}$$

hence the pdf is properly normalized, while

$$I_1 = \langle E \rangle = \frac{2}{\beta}(1+\alpha). \tag{25}$$

Now, realizing that the energy variable E is normalized with the variance of the signal one would expect that the average value of E should be equal to 1. This then gives the following relation between α and β, i.e.

$$\beta = 2(1+\alpha). \tag{26}$$

Another relation between α and β is obtained by matching the empirical CDF (18) with the theoretical one, given in Eq. (9), which is denoted by P_{th}. The fitting constant α then follows from the condition that at the edge of the range of validity, taken as $E_b = 10$ (corresponding to $h = 2.2$), the empirical CDF equals the theoretical one, i.e. $P(E_b) = P_{th}(E_b)$. This gives for α, eliminating β using (26),

$$\alpha = \frac{f_b^2 - 2E_b}{2(E_b + f_b)},\ f_b = \log P_{th}(E_b). \tag{27}$$

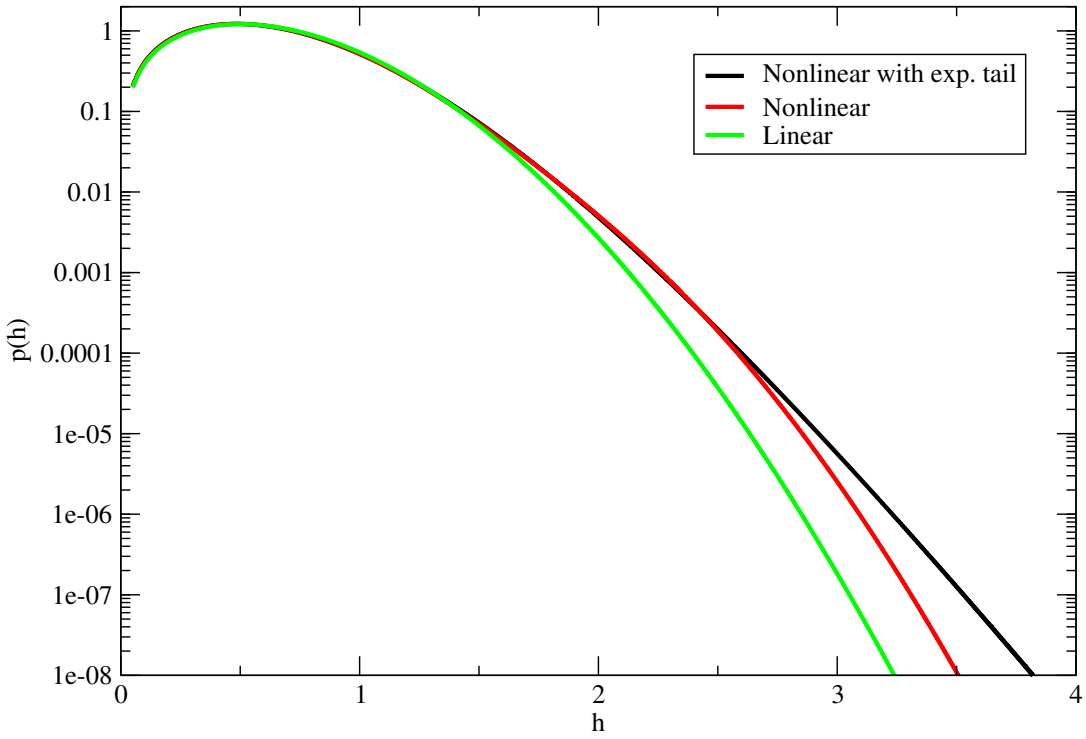

Figure 4: Pdf of envelope wave height for the Draupner freak wave event at 16:00 hrs. The black line corresponds to the empirical approach where α and β have been matched using (26) and (27). The red line corresponds to the theoretical pdf, while the green line corresponds to linear theory.

where f_b is the logarithm of the theoretical CDF at the boundary given by $E = E_b$. In this manner a connection between skewness and kurtosis of the sea state, via f_b, and the fitting parameters of the empirical CDF has been established. For relatively small values of C_4 and C_3 this matching procedure seems to be working well. As an illustration, I show in Fig. 4 the result of the matching procedure applied to the most extreme stats of the Draupner case at 16:00 hrs. The empirical form shows a gradual transition from a Gaussian pdf to an exponential pdf. When the results are plotted on a linear scale (not shown), it is seen that the empirical pdf (18) gives a perfect match with the theoretical result in the range of h-values from 0 to 2. Clearly, nonlinear effects are only relevant for extreme values of the dimensionless envelope wave height. In addition, I inspected for this case what is the main contributor to the deviations from the Gaussian distribution, effects of skewness or kurtosis. In this case it turns out that both skewness and kurtosis contribute but the impact of kurtosis on the deviations from Normality is slightly larger.

3 How rare is the Draupner wave event?

We have now developed all the necessary ingredients to be able to do the next step, that is try to assess how likely the Draupner freak wave event is. The present approach is based on a statistical representation of the sea state in terms of the wave spectrum. Therefore, it is assumed that the wave spectrum gives an

average description of the sea state in a domain of the size of $L_x \times L_y$ km^2 surrounding the grid point of interest, where L_x and L_y are the distance between two gridpoints in the x- and y direction, respectively. For the present simulation of the waves the spatial resolution is 10 km, therefore $L_x = L_y = 10$ km. Making use of the spectrum we are then able to obtain the ensemble averaged probability distribution function for envelope wave height and linear wave energy. The question then is how likely will the Draupner freak wave event be considering a domain size of 10×10 km^2. To be more specific we are going to determine the probability that in the domain in question maximum envelope wave height is equal or larger than the observed value at the Draupner platform. In order to achieve this we need to obtain the maximum wave height pdf and we need an estimate of the number of events in a spatial domain of given size.

Goda (2000) obtained the maximum wave height distribution from a (time) series of N wave events. Here we use Goda's (2000) approach but now applied to a spatial series of the envelope wave height. Introducing the function

$$\mathscr{G}(h) = -NP(h),$$

which, apart from a minus sign, equals to the product of the number of events N and the cumulative distribution

$$P = \int_h^\infty \mathrm{d}h \; p(h),$$

we have for the maximum envelope wave height distribution

$$p_{max}(h = h_{max}) = \frac{\mathrm{d}\mathscr{G}}{\mathrm{d}h} \exp(\mathscr{G}). \tag{28}$$

Close inspection of this result shows that this distribution is a double exponential function in general, but for large maximum envelope wave heights (typically of the order of 2 or larger) the pdf simplifies considerable because it becomes

$$p_{max}(h) = N \; p(h).$$

Now the probability that maximum envelope wave height equals or exceeds a given observed value, denoted by h_{max}^{obs}, is given by

$$P_{ex}(h_{max}^{obs}) = \int_{h_{max}^{obs}}^\infty \mathrm{d}h \; p_{max}(h) = 1 - \exp(-NP(h_{max}^{obs})) \tag{29}$$

and the main task is how to choose the number of events. Janssen (2015) has studied this issue extensively for time series. To that end one needs to define what an event is. It is customary to define an event with respect to a reference level h_c, therefore an event starts where the envelope has an upcrossing and finishes at the next downcrossing. The frequency of events is then determined by the upcrossing frequency, and N then equals the product of the upcrossing frequency and the length T_L of the timeseries. However, the frequency of events depends on the chosen reference level, and, therefore it may be more appropriate to introduce an average frequency. Janssen (2015) took as measure the average of the rate of change of h with time, $\dot{h}$, normalized with h itself. The averaging is done using the joint pdf of h and $\dot{h}$ which for a Gaussian sea state can be easily obtained from the joint pdf of envelope ρ and phase θ and its time derivatives (see e.g. Janssen, 2014). Performing the averaging one finds for the average upcrossing frequency

$$\langle f_{up} \rangle = \langle \dot{h}/h \rangle = \nu \bar{\omega}, \tag{30}$$

where $\bar{\omega}$ is the mean angular frequency, determined by the ratio of the first and zeroth moment of the spectrum, $\bar{\omega} = m_1/m_0$, while ν is the spectral width parameter defined as $\nu = (m_0 m_2/m_1^2 - 1)^{1/2}$. When

analyzing timeseries in terms of the envelope, the frequency scale $\nu\bar{\omega}$, which corresponds to the inverse of the timescale of the wave groups, is introduced in a natural way. The number of envelope events N is therefore, as expected, related to the number of wave groups, thus

$$N = \nu\bar{\omega}\, T_L, \tag{31}$$

and for this choice of the number of events good agreement between the maximum wave height pdf and Monte Carlo simulations of a Gaussian sea state was reported. In particular, it was shown that the expected maximum envelope wave height scales with N while it does not scale with the number of waves $N_w = T_L/T_P$ (with T_P the peak period) in the time series.

One would expect that the analysis of the number of events in a spatial domain can be done following a similar approach.[2] It would therefore be most natural to estimate N by determining the average up-crossing wavenumber using $\langle h_x/h\rangle$. Formally this can be done and a similar result will be found as the one in (29), but the width of the wavenumber spectrum $\mu = (m_0 m_2/m_1^2 - 1)^{1/2}$ involves moments of the wavenumber spectrum. Unfortunately, the second moment m_2 is in this case not well-defined because the high-wavenumber tail of the spectrum scales like k^{-3} and therefore the second moment has a logarithmic singularity.

I therefore decided to estimate the number of events in a slightly different fashion. Consider a wave spectrum and rotate it in such a way that the mean wave direction is in the x-direction. The wavenumbers k_x and k_y are then given by

$$k_x = k\cos\theta,\; k_y = k\sin\theta.$$

and the width in the x-direction and y-direction is obtained by a Taylor expansion of the wavenumbers around the vector $\mathbf{k} = (k_x, 0)$. Hence,

$$\delta k_x = \delta k,\; \delta k_y = k\delta\theta.$$

where $\delta\theta$ is basically the directional width of the spectrum σ_θ, while the width in the wavenumber spectrum follows from the relation $\delta k = \partial k/\partial\omega \times \delta\omega$. Thus for deep water the relative width of the wave number spectrum becomes $\sigma_k = \delta k/k = 2\delta\omega/\omega = 2\sigma_\omega$, or, since the group velocity $v_g = \partial\omega/\partial k$ is half the phase speed $c = \omega/k$, the width in wavenumber space is twice the width in frequency space. All in all, the number of events on the two-dimensional surface becomes

$$N_{2D} = 2\sigma_\theta/\sigma_\omega \times N^2. \tag{32}$$

where N is given in (31) and I have chosen the duration in such a way that it matches the domain size, i.e. $T_L = L_x/v_g$. Using the above expression for the number of events it should be noted that in a domain of 10×10 km^2 the number of events is quite large, for the Draupner event I typically find $N = 350{,}000$.

Note that for the Draupner cases considered the directional width σ_θ is typically 2-3 times larger then the width σ_ω in the frequency direction. Assuming that the ECWAM wave model is properly modelling the directional width, it is therefore unlikely that for the Draupner case nonlinear focussing caused by the Benjamin-Feir instability plays a dominant role. In addition, it should be noted that the Draupner

[2] That is, if one estimates the number of 'independent' events in the x-direction by N_x and in the y-direction by N_y the total number of events is $N_{2D} = N_x \times N_y$, and the probability of the 'extreme' event is proportional to N_{2D}. However, an argument from the field of Topology (for an accesible reference see Worsley, 1996) suggests that the chance on an extreme event in $2D$ is considerable larger. Probabilities for extreme events in 2D in this work are therefore underestimated. This theorem from Topology is based on an Gaussian sea surface and work to extend this into the nonlinear regime still needs to be done. Nevertheless, a number of researchers (see e.g. Baxevani and Richlik, 2004; Fedele, 2012; Benetazzo *et al.*, 2015) have applied this approach to obtain the recurrence probability of extreme events.

location has a water depth D of 69 m and at the time the freak wave event happened the wave spectrum had quite low frequencies in such a way that $k_pD = 1.45$ which is close to the value of the dimensionless wavenumber, i.e. $k_pD = 1.363$, where according to Janssen and Onorato (2007) the nonlinear transfer coefficient $T_{1,2,3,4}$ of Eq. (8) vanishes.

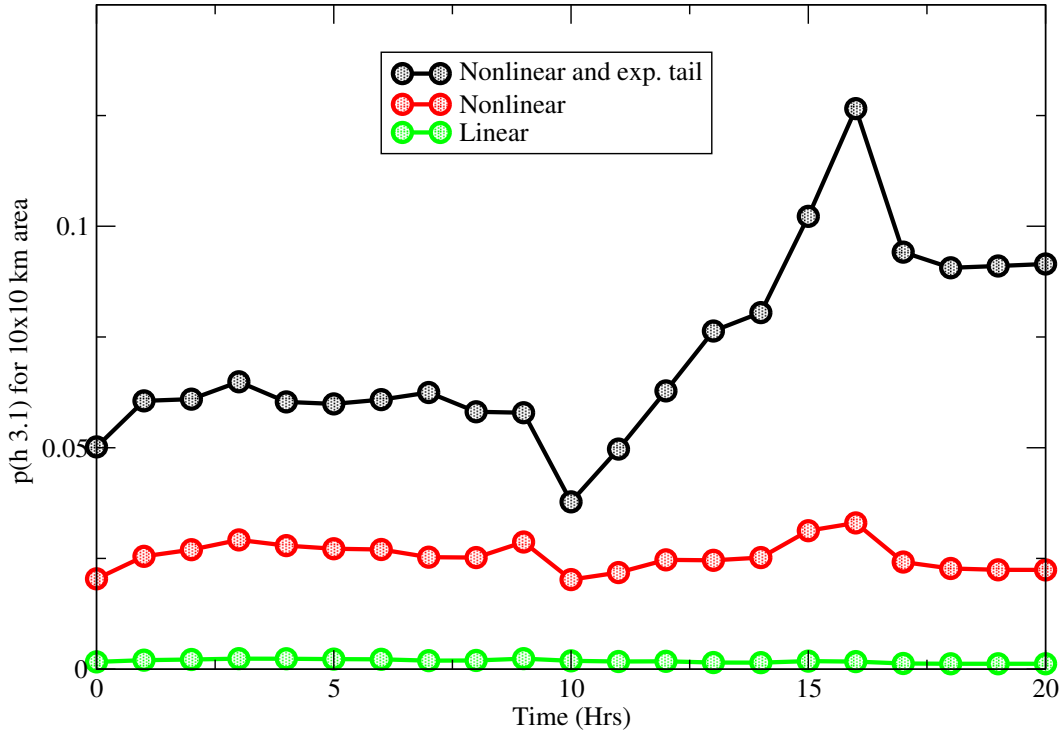

Figure 5: Evolution in time of simulated exceedance probability $P_{ex}(h^{obs}_{max})$ for $h^{obs}_{max} = 3.1$. Location is the Draupner platform on the 1^{rst} of January 1995.

Combining everything together I show in Fig 5 the time series of the exceedance probability given in Eq. (29), where I have chosen for observed dimensionless maximum wave height $h^{obs}_{max} = 3.1$. Three case are shown, probabilities using linear theory (green), nonlinear theory (red) and nonlinear theory with an exponential tail (black). It is seen, according to nonlinear theory with exponential tail added, that for the given domain it is fairly likely that the freak wave event could have occurred in the Draupner area. According to linear theory, on the other hand, this seems not very likely.

Compared to standard nonlinear theory, the addition of the exponential tail has increased probabilities by a factor of 3-4. I think this is quite substantial, but it will only happen when the event is really extreme, such as the Draupner event. Furthermore, with some optimism in mind, it could be argued that there is some evidence that the freak wave event should have most likely occurred around 15:00-16:00 hrs in the afternoon simply because the exceedance probability is maximum at that time. This is probably not a very scientific statement. However, note that from 10:00 and onwards the exceedance probability is gradually increasing towards its maximum. Because of the sudden drop from 9:00 to 10:00 I have tried to understand why the shape of the 10:00 spectrum is so special, but so far I have not succeeded to understand this. The time evolution of the expectation value of maximum wave height, as shown in Fig.

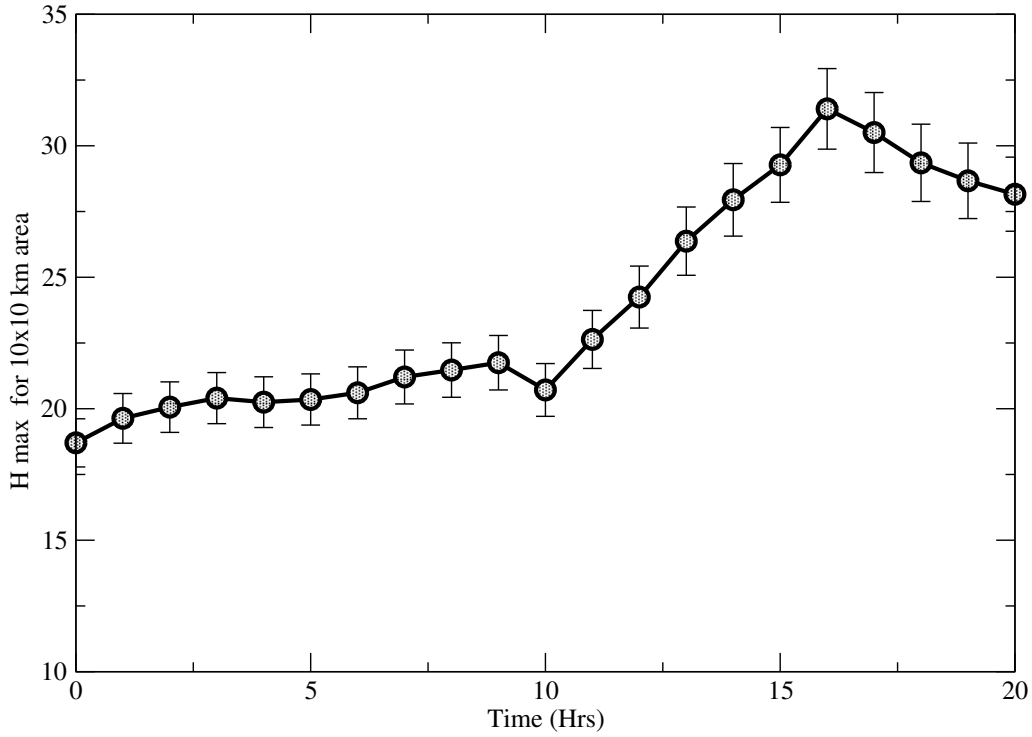

Figure 6: Evolution in time of simulated expectation value of maximum envelope wave height at the Draupner platform on the 1^{rst} of January 1995. The observed maximum is about 37 m

6, suggests, however, that this might be related to a sudden strengthening of the wind at that time.

Finally, it is important to realize that a realistic simulation of an extreme event such as discussed in this note is only possible using a high-resolution forecasting system. In order to illustrate this point I show in Fig. 7 a comparison of exceedance probabilities obtained from the new high-res system (with spatial resolution of 9 km) with results from a low-resolution (25 km) version of the ERA-interim analysis and forecasting system. It is clear that from the low-resolution system there is virtually no indication that there is an extreme event around 15:00 hours in the afternoon, while results from the high-resolution system seem to give some indication. I suspect that this is connected to the ability of the high-resolution system to generate a small-scale polar low that resulted in quite strong winds when the Draupner event occurred (cf. Fig. 8). Comparing the sea state from the two simulations it turns out that in the high-resolution system wave height was considerable higher (11.24 m vs. 9.43 m), while waves were considerably longer and steeper (an increase in steepness of 10%) and therefore shallow water effects were much more important (k_pD = 1.45 versus 1.7). Although, as already remarked, the dynamical part of the kurtosis tends to get reduced in shallow waters, the opposite is the case for the bound-wave part of the envelope kurtosis. Combined with the larger steepness in the high-resolution simulation one finds a substantial increase in kurtosis around 15:00 hours as shown in Fig. 3, while there is hardly any increase in envelope kurtosis in the low-resolution simulation. Therefore, for extreme events spatial resolution matters.

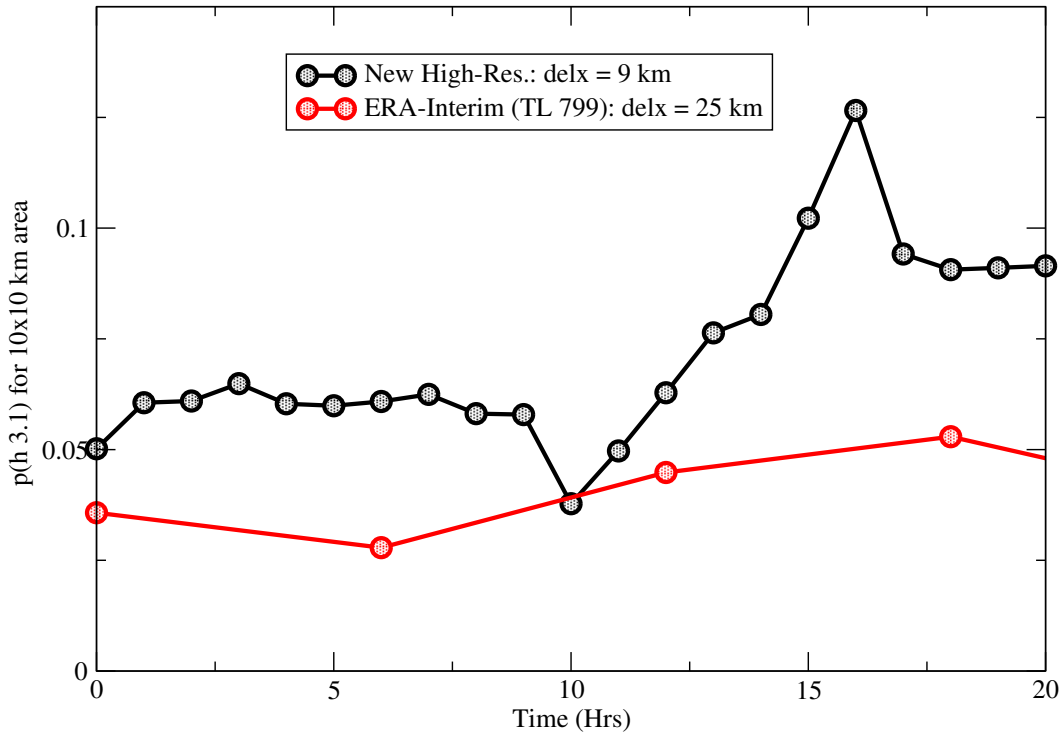

Figure 7: Evolution in time of simulated exceedance probability $P_{ex}(h^{obs}_{max})$ for $h^{obs}_{max} = 3.1$. Location is the Draupner platform on the 1^{rst} of January 1995.

4 Conclusions.

ECMWF is developing a new higher resolution weather and wave forecasting system and this experimental version has been applied to the simulation of the Draupner freak wave event. This simulation was quite succesful since it picked up a small scale polar low which played an important role in the sea state generation at the time the freak wave event occurred in the Draupner platform area. Nevertheless, simulated significant wave height at the time of the incident was somewhat smaller than observed, namely 11.24 versus 12 m.

Ocean wave forecasting is about forecasting of the ensemble mean state as characterized by the predicted wave spectrum. In this note I have adopted the interpretation that the wave spectrum represents the mean sea state in a domain surrounding the location of interest with a size given by the spatial resolution of the wave forecasting system. Deviations from the mean state are given by the probability distribution function of, for example, the envelope wave height. Deviations from Normality are determined from the mean sea state and therefore the pdf represents the statistics of the same domain. On the other hand, freak waves are a singular event. They are caused by a combination of constructive interference augmented by a number of nonlinear effects (for example effects related to skewness and kurtosis and related to nonlinear focussing by the Benjamin-Feir instability) and by the presence of currents. However, their starting point is constructive interference (which was already extensively discussed by Janssen (2003)) and therefore we are clearly dealing with the luck of the draw in the lottery as there is no a priory

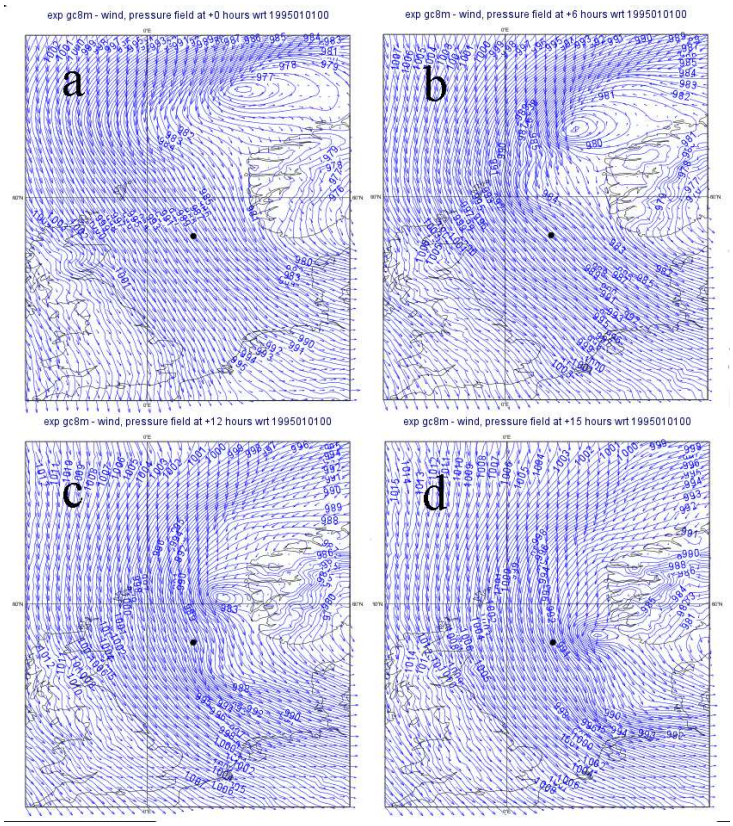

Figure 8: Forecast surface pressure and wind for the Draupner event. Start date of the forecast is at midnight of the 1^{rst} of January 1995. The location of the Draupner platform is shown by the dot. At 15:00 hours the small scale polar low squeezes the isobars to produce considerably strong winds at Draupner, generating, according to the wave model a mean sea state with significant wave height of 11.24 m.

knowledge of the phases of the waves. In the context of an ensemble wave prediction system it is therefore not possible to validate its results against individual singular events such as freak waves are. At best one may try to answer the question how likely the observed event is given the simulated probability distribution function. In other words, what is the exceedance probability that the observed event occurs in the domain matching the resolution of the wave prediction system. In this note I have tried to answer this question and it is found that if one assumes linear theory than it is very unlikely that the Draupner wave event could have happened. In sharp contrast to this, when nonlinear effects such as skewness and kurtosis are included (augmented with an exponential tail) then the Draupner freak wave event seems to be quite likely. Note that both skewness and kurtosis effects are contributing to a better explanation of this event.

It is emphasized that still work needs to be done to extend the development to estimate the occurrence probability of extreme events in 2D+Time. This work was started by J. Adler (1981) who used insights from Topology to provide an upper estimate of this probability for a Gaussian surface evolving in time. Clearly, these insights need to be applied to the envelope signal, including nonlinear effects. For example, referring to Baxevani and Rychlik (2006), the recurrence probability should depend in general on

moments of the wavenumber-frequency spectrum, which reduces to moments of the usual frequency-direction spectrum when it is assumed that there are only free waves present. In the presence of bound waves these moments become evidently more involved (cf. Janssen, 2009)

Finally, the Draupner freak wave event occured during a fairly rapid generation of wind sea while the winds were getting stronger. Wind seas normally are short crested which means that they are broader in direction than in frequency. This short crestness of the sea state tends to reduce the effectiveness of the nonlinear focussing by the Benjamin-Feir instability, so most likely this mechanism was not so effective. However, according to the simulation results shown in Fig. 2 the excess kurtosis $\langle \eta^4 \rangle / \langle \eta^2 \rangle^2 - 3$ was still of the order of 0.1 and gave a significant contribution to the tail of the pdf. Nevertheless, this nonlinear focussing is expected to be more effective in cases of strong swells that may become long crested in the course of time.

Acknowledgement.

Discussions with Miguel Onorato and Stefania Residori are greatly appreciated. Miguel Onorato was kind enough to determine the Hilbert transform of the Draupner wave event.

Appendices.

A Skewness and Envelope kurtosis.

In this Appendix I will sketch the derivation of all relevant statistical moments, namely the variance, the skewnes and the envelope kurtosis. For the Stokes wave train the results have been validated against Monte Carlo simulations of the envelope wave height distribution. These simulations also show that for extreme events the pdf is indeed exponential. Residori's function seems to fit the simulated data very well.

We need to evaluate the variance of the surface elevation η and its Hilbert transform ζ and we also need to evaluate a number of skewness terms and the envelope kurtosis. Recall that

$$\eta = \frac{1}{2}(Z+Z^*), \text{ and } \zeta = \frac{1}{2i}(Z-Z^*),$$

Following Janssen (2014) the complex function Z is obtained from the canonical transformation by collecting together terms of similar time-asymptotic behaviour, i.e. Z contains all the terms that vanish for $\Im(t) \rightarrow -\infty$. The canonical transformation is only known as an expansion in steepness ε so we write $Z = \varepsilon Z_1 + \varepsilon^2 Z_2 + \varepsilon^3 Z_3$ with

$$Z_1 = 2\int_{-\infty}^{\infty} \mathrm{d}\mathbf{k}_1 \; f_1 a_1 \; e^{i\theta_1}, \tag{A1}$$

where $f_1 = (\omega_1/2g)^{1/2}$, $\theta_1 = \mathbf{k}_1 \cdot \mathbf{x}$, and

$$Z_2 = 2\int_{-\infty}^{\infty} \mathrm{d}\mathbf{k}_{1,2,3} \; f_2 f_3 \; e^{i\theta_1} \left\{ \mathscr{A}_{2,3} a_2 a_3 \delta_{1-2-3} + 2\mathscr{B}_{2,3} a_2^* a_3 H_{3-2} \delta_{1+2-3} \right\}, \tag{A2}$$

while

$$Z_3 = 2\int \mathrm{d}\mathbf{k}_{1,2,3,4} f_2 f_3 f_4 e^{i\theta_1} \{ \mathscr{D}_{1,2,3,4} a_2 a_3 a_4 \delta_{1-2-3-4} + \mathscr{C}_{1,2,3,4} a_2 a_3 a_4^* \delta_{1-2-3+4} H_{2+3-4} + \mathscr{C}_{-1,2,3,4} a_2^* a_3^* a_4 \delta_{1+2+3-4} H_{4-3-2} \}. \tag{A3}$$

The interaction coefficients $\mathscr{A}, \mathscr{B}, \mathscr{C}$, and $\mathscr{D}$ are defined in Janssen (2009). The Heaviside function $H(x)$ is defined in such a way that $H(0) = 1/2$ and in the above formulae the argument of the Heaviside function is a sum of angular frequencies, e.g. $H_{3-2} = H(\omega_3 - \omega_2)$.

As noted in Janssen (2009) the quadratic part of the canonical transformation and therefore also of Z generates a mean sea level. In other words, while $\langle Z_1 \rangle$ and $\langle Z_3 \rangle$ vanish this is not the case for $\langle Z_2 \rangle$. In fact one finds

$$\langle Z_2 \rangle = \int_{-\infty}^{\infty} \mathrm{d}\mathbf{k}_1 \mathscr{B}_{1,1} E_1,$$

and the ensemble mean average sea level will be substracted from the the surface elevation signal η so that the corrected signal has no bias. Note that the Hilbert transform ζ of the signal has by construction always a vanishing mean, in agreement with the property that the Hilbert transform of a constant vanishes.

Finally, at this point I would also like to record the corresponding results for the case of a single wave train. It turns out that, in practice, the narrow-band limit serves as a reasonable approximation to the case of general spectra, so that these simplified results may be used in the operational implementation of the

pdf of extreme events. The wave train is given by the Stokes wave solution up to third order in amplitude that is consistent with the narrow-band approximation for the general case of arbitrary spectra.

The narrow-band limit follows in a straightforward fashion from the complex function Z by using a wavenumber spectrum with a Dirac delta function, i.e. $E(\mathbf{k}) = m_0\delta(\mathbf{k}-\mathbf{k}_0)$ where m_0 is the variance of the sea surface, and $\mathbf{k}_0$ is the peak wave number. In effect, all the interaction coefficients are replaced by their value at the peak wave number. Writing

$$\mathscr{A}_{0,0} = 2\alpha, \mathscr{B}_{0,0} = 2\Delta, \mathscr{C}_{0,0,0,0} = 4\gamma, \text{ and } \mathscr{D}_{0,0,0,0} = 4\beta, \tag{A4}$$

the complex function Z becomes

$$Z = m_0 D + m_0^{1/2} A e^{i\theta} + m_0 B e^{2i\theta} + m_0^{3/2} C e^{3i\theta}, \tag{A5}$$

with $D = \Delta(a^2 - \langle a^2\rangle), A = a(1+\gamma\varepsilon^2 a), B = \alpha a^2, C = \beta a^3$, and $\theta = k_0 x - \omega_0 t + \phi$, with ω_0 the angular peak frequency and ϕ an arbitrary phase. The coefficients α, β, γ and Δ are known functions of peak wavenumber and depth h and they read

$$\Delta = -\frac{k_0}{4}\frac{c_S^2}{c_S^2 - v_g^2}\left[\frac{2(1-T_0^2)}{T_0} + \frac{1}{x}\right], \; \alpha = \frac{k_0}{4T_0^3}\left(3 - T_0^2\right),$$

$$\beta = \frac{3k_0^2}{64T_0^6}\left[8 + \left(1-T_0^2\right)^3\right], \; \gamma = -\frac{1}{2}\alpha^2, \tag{A6}$$

where $x = k_0 h$, $T_0 = \tanh x$, $c_S^2 = gh$, $v_g = \partial\omega/\partial k$, and $\omega_0 = (gk_0T_0)^{1/2}$. I have used the form (A5) to calculate explicitely all the relevant statistical moments following the method in Janssen (2009, Appendix A.3), and I have found complete agreement with the narrow-band limit of the results for general spectra. Note that in these calculations I have assumed a certain ordering of the contributions to the surface elevation. Introducing the significant steepness $\varepsilon = k_0 m_0^{1/2}$, with typical magnitude in the range 0.01-0.05, one finds that the constant term in (A5) is of order ε^2 while the first, second and third harmonic are of order ε, ε^2 and ε^3 respectively. Calculations of the statistical moments will be performed up to lowest significant order, which means that I continue the calculation up to the first nontrivial contribution of nonlinearity.

A.1 Variance.

It is straightforward to express the variances $\langle\eta^2\rangle$ and $\langle\zeta^2\rangle$ in terms of the complex envelope function Z. The result becomes

$$\langle\eta^2\rangle = \frac{1}{2}\left(\langle|Z|^2\rangle + \langle Z^2\rangle\right), \; \langle\zeta^2\rangle = \frac{1}{2}\left(\langle|Z|^2\rangle - \langle Z^2\rangle\right). \tag{A7}$$

For a homogeneous, Gaussian sea state the variances become to lowest significant order

$$\langle\eta^2\rangle = \int d\mathbf{k}_1 \, E_1 + \int d\mathbf{k}_{1,2} E_1 E_2 \left\{\mathscr{A}_{1,2}^2 + \mathscr{B}_{1,2}^2 + 2\mathscr{C}_{1,1,2,2}\right\},$$

$$\langle\zeta^2\rangle = \int d\mathbf{k}_1 \, E_1 + \int d\mathbf{k}_{1,2} E_1 E_2 \left\{\mathscr{A}_{1,2}^2 + \mathscr{B}_{1,2}^2 (H_{1,2} - H_{2,1})^2 + 2\mathscr{C}_{1,1,2,2}\right\}. \tag{A8}$$

The expression for the variance $\langle\eta^2\rangle$ agrees with an earlier result obtained in Janssen (2009, Eq. (50)). Note that formally the variance of ζ may differ from the variance of η, because of the presence of the

additional factor $F_{1,2} = (H_{1,2} - H_{2,1})^2$. The function $F_{1,2}$ equals 1 everywhere except when its arguments are equal. In that event $F_{1,1}$ vanishes. However, if the remainder of the integrand is continuous then removing a point from an integral should not affect the result. Hence, for continuous spectra the variance of η and ζ are the same. The exception is when the remainder of the integrand is singular at the point that is being removed. An example of this is the case of a single wave which has a delta function spectrum. As a consequence, for the single wave case the variances of η and ζ are different. In fact, taking the narrow-band limit of (A8) one finds using Eq. (A4)

$$\langle \eta^2 \rangle = m_0 + 4m_0^2 \left(2\gamma + \alpha^2 + \Delta^2\right), \; \langle \zeta^2 \rangle = m_0 + 4m_0^2 \left(2\gamma + \alpha^2\right), \tag{A9}$$

and the variances differ by the amount $4m_0^2\Delta^2$. Expression (A9) is in agreement with the single mode results using Eq. (A5). Note that from the expression of the single mode complex envelope function it is immediately clear that the variance of ζ cannot depend on the parameter Δ, since the Hilbert transform of a constant vanishes.

A.2 Skewness.

We need to evaluate skewness terms for the surface elevation η and its Hilbert transform ζ. In terms of the complex function Z one finds

$$\langle \eta^3 \rangle = \frac{1}{8}\left(\{\langle Z^3 \rangle + 3\langle |Z|^2 Z \rangle\} + c.c., \; \langle \eta^2 \zeta \rangle = \frac{1}{8i}\left\{\langle Z^3 \rangle + \langle |Z|^2 Z \rangle - c.c.\right\},\right.$$

while

$$\langle \eta \zeta^2 \rangle = \frac{1}{8}\left\{\langle |Z|^2 Z \rangle - \langle Z^3 \rangle\right\} + c.c., \; \langle \zeta^3 \rangle = \frac{i}{8}\left\{\langle Z^3 \rangle - 3\langle |Z|^2 Z \rangle - c.c.\right\}.$$

so we only have to evaluate the moments $\langle Z^3 \rangle$ and $\langle |Z|^2 Z \rangle$. To lowest significant order in ε we only need the first two terms of the complex function Z, i.e. (A1)-(A2), Then, by invoking the random phase approximation it is straightforward to establish that

$$\langle Z^3 \rangle = 0 + \mathscr{O}(\varepsilon^5), \; \langle |Z|^2 Z \rangle = 4 \int \mathrm{d}\mathbf{k}_{1,2} \left(\mathscr{A}_{1,2} + \mathscr{B}_{1,2}\right) E_1 E_2 + \mathscr{O}(\varepsilon^5), \tag{A10}$$

where $\mathscr{A}_{1,2}$ and $\mathscr{B}_{1,2}$ are given in Janssen (2009). Hence, the Z-moments either vanish or are real. The direct consequence is that the surface elevation moments involving odd powers of ζ vanish, i.e. $\langle \eta^2 \zeta \rangle = \langle \zeta^3 \rangle = 0$. The remaining moments become

$$\langle \eta^3 \rangle = 3 \int \mathrm{d}\mathbf{k}_{1,2} E_1 E_2 \left(\mathscr{A}_{1,2} + \mathscr{B}_{1,2}\right), \; \langle \eta \zeta^2 \rangle = \frac{1}{3}\langle \eta^3 \rangle. \tag{A11}$$

The eventual result is

$$\kappa_{30} = \frac{3}{m_0^{3/2}} \int \mathrm{d}\mathbf{k}_{1,2} E_1 E_2 \left(\mathscr{A}_{1,2} + \mathscr{B}_{1,2}\right), \; \kappa_{12} = \frac{\kappa_{30}}{3}, \tag{A12}$$

while κ_{21} and κ_{03} vanish. Hence, the skewness terms for general spectra share the same properties as the skewness terms for a single wave train in deep water (Janssen, 2014). Note that in the narrow-band limit the skewness term κ_{30} assumes the simple form

$$\kappa_{30} = 6m_0^{1/2}\left(\alpha + \Delta\right), \tag{A13}$$

a result which is in agreement with Janssen (2009).

Finally, in the envelope wave height pdf we have introduced a skewness factor C_3 according to Eq. (6). Making use of the properties of the skewness terms one finds eventually

$$C_3 = \frac{\kappa_{30}}{3}, \tag{A14}$$

and this expression for C_3 has been used to determine the skewness factor in the wave height pdf from the simulated spectra.

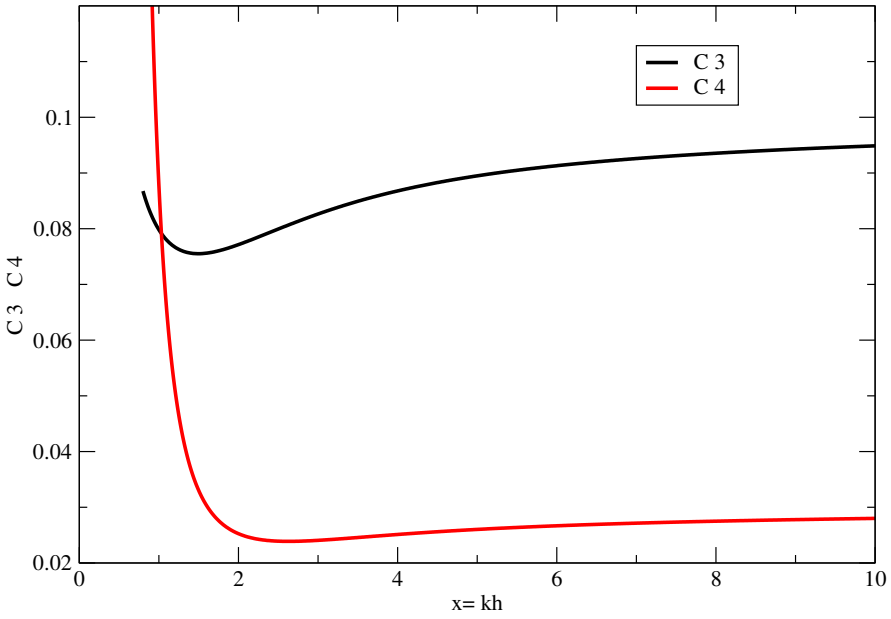

Figure 9: Dependence of skewness factor C_3 and kurtosis factor C_4 on dimensionless depth x according to the single mode results.

A.3 Kurtosis.

The procedure to obtain the fourth cumulants of surface elevation η and its Hilbert transform ζ, i.e.

$$\kappa_{40} = \frac{\langle \eta^4 \rangle}{\langle \eta^2 \rangle^2} - 3, \; \kappa_{22} = \frac{\langle \eta^2 \zeta^2 \rangle}{\langle \eta^2 \rangle \langle \zeta^2 \rangle} - 1, \; \kappa_{04} = \frac{\langle \zeta^4 \rangle}{\langle \zeta^2 \rangle^2} - 3, \tag{A15}$$

is formally the same as the one used to obtain the third cumulants such as the skewness of the surface elevation. Again, one introduces the complex function Z but it is now more involved because of third-order nonlinearity, i.e. $Z = \varepsilon Z_1 + \varepsilon^2 Z_2 + \varepsilon^3 Z_3$, where Z_1, Z_2 and Z_3 are given by (A1), (A2) and (A3) respectively.

The main purpose is to calculate the envelope kurtosis κ_4. It is defined as

$$\kappa_4 = \kappa_{40} + 2\kappa_{22} + \kappa_{04}, \tag{A16}$$

where the surface elevation kurtosis terms are given by Eq. (A15). This means we have to evaluate $\langle \eta^4 \rangle, \langle \eta^2 \zeta^2 \rangle$, and $\langle \zeta^4 \rangle$.

In passing, I would like to explain why κ_4 is called the envelope kurtosis. This is most easily illustrated for the case that η and ζ have the same variance, which is true for continuous spectra. From the definition (A16), while using the definitions of κ_{40}, κ_{22}, and κ_{04} it is then straightforward to show that the envelope kurtosis κ_4 is just given, as expected, by the normalized fourth moment of the envelope $\rho = \sqrt{\eta^2 + \zeta^2}$, i.e.

$$\kappa_4 = \frac{\langle \rho^4 \rangle}{\langle \eta^2 \rangle^2} - 8, \tag{A17}$$

In terms of the complex function Z we therefore have

$$\kappa_4 = \frac{\langle |Z|^4 \rangle}{\langle \eta^2 \rangle^2} - 8, \tag{A18}$$

hence, in order to obtain the envelope kurtosis one only needs to determine the fourth moment $\langle |Z|^4 \rangle$. However, for the single mode case η and ζ do not have the same variance and therefore the expression (A18) might not always be valid. For completeness, therefore, I will evaluate all the relevant surface elevation moments given in (A15). Then, in terms of Z the fourth moments become

$$\begin{aligned} \langle \eta^4 \rangle &= \frac{1}{16} \left(\langle Z^4 \rangle + 4 \langle Z^3 Z^* \rangle + 3 \langle |Z|^4 \rangle + c.c. \right), \\ \langle \eta^2 \zeta^2 \rangle &= \frac{1}{16} \left(\langle |Z|^4 \rangle - \langle Z^4 \rangle + c.c. \right), \end{aligned}$$

and

$$\langle \zeta^4 \rangle = \frac{1}{16} \left(\langle Z^4 \rangle - 4 \langle Z^3 Z^* \rangle + 3 \langle |Z|^4 \rangle + c.c. \right), \tag{A19}$$

hence these moments depend on combinations of $\langle Z^4 \rangle, \langle Z^3 Z^* \rangle$ and $\langle |Z|^4 \rangle$. For equal variance it is clear from the above expressions that by adding the first and the last term and by adding twice the second term the envelope kurtosis only involves the moment $\langle |Z|^4 \rangle$, which confirms the result (A18).

It is now a straightforward but very laborious task to evaluate the above Z-moments for a homogeneous, Gaussian sea state. The eventual result is

$$\begin{aligned} \langle |Z|^4 \rangle = 8 \int \mathrm{d}\mathbf{k}_{1,2} E_1 E_2 + 32 \int \mathrm{d}\mathbf{k}_{1,2,3} E_1 E_2 E_3 \Big\{ & \mathscr{C}_{1,1,2,2} + \frac{1}{2} \mathscr{C}_{1+2-3,1,2,3} H_{1+2-3} + \mathscr{A}_{1,2} \mathscr{A}_{2,3} \\ & + \mathscr{A}_{2,1} \mathscr{B}_{1,3} + \frac{1}{2} \mathscr{A}_{2,3}^2 + \frac{1}{2} \mathscr{B}_{2,3}^2 (H_{2-3}^2 + H_{3-2}^2) + \mathscr{B}_{1,3} \mathscr{B}_{3,2} \left[H_{3-2} H_{3-1} + H_{2-3} H_{1-3} \right] \Big\} \end{aligned}$$

$$\begin{aligned} \langle Z^3 Z^* \rangle = 12 \int \mathrm{d}\mathbf{k}_{1,2,3} E_1 E_2 E_3 \{ & \mathscr{D}_{1+2+3,1,2,3} + \mathscr{C}_{1+2-3,1,2,3} H_{3-2-1} + 2 \mathscr{A}_{2,3} \mathscr{B}_{3,1} \\ & + 4 \mathscr{B}_{3,1} \mathscr{B}_{1,2} H_{1-3} H_{2-1} + 2 \mathscr{B}_{1,2}^2 H_{1-2} H_{2-1} \} \end{aligned}$$

while $\langle Z^4 \rangle$ vanishes. We now substitute the Z-moments into the expressions (A19) and using the variances (A9) one finds to lowest significant order the following expressions for the fourth-order cumulants

$$\kappa_{40} = \frac{12}{m_0^2} \int \mathrm{d}\mathbf{k}_{1,2,3} E_1 E_2 E_3 \left\{ \left(\mathscr{A}_{1,3} + \mathscr{B}_{1,3} \right) \left(\mathscr{A}_{2,3} + \mathscr{B}_{2,3} \right) + \frac{1}{2} \mathscr{C}_{1+2-3,1,2,3} + \frac{1}{2} \mathscr{D}_{1+2+3,1,2,3} \right\} \tag{A20}$$

$$\begin{aligned} \kappa_{22} = \frac{4}{m_0^2} \int \mathrm{d}\mathbf{k}_{1,2,3} E_1 E_2 E_3 \Big\{ & \mathscr{A}_{1,2} \mathscr{A}_{2,3} + \mathscr{A}_{1,2} \mathscr{B}_{2,3} + \frac{1}{2} \mathscr{C}_{1+2-3,1,2,3} H_{1+2-3} \\ & + \mathscr{B}_{1,3} \mathscr{B}_{3,2} \left[H_{3-2} H_{3-1} + H_{2-3} H_{1-3} \right] \} \end{aligned} \tag{A21}$$

and

$$\kappa_{04} = \frac{12}{m_0^2}\int \mathrm{d}\mathbf{k}_{1,2,3}E_1E_2E_3\left\{\mathscr{A}_{1,2}\mathscr{A}_{2,3}+\mathscr{B}_{1,3}\mathscr{B}_{3,2}\left[H_{3-2}H_{3-1}+H_{2-3}H_{1-3}-2H_{3-1}H_{2-3}\right]\right.$$
$$\left.+\frac{1}{2}\mathscr{C}_{1+2-3,1,2,3}(H_{1+2-3}-H_{3-2-1})-\frac{1}{2}\mathscr{D}_{1+2+3,1,2,3}\right\} \quad \text{(A22)}$$

As a consequence, the envelope kurtosis becomes

$$\kappa_4 = \frac{32}{m_0^2}\int \mathrm{d}\mathbf{k}_{1,2,3}E_1E_2E_3\left\{\mathscr{A}_{1,2}\mathscr{A}_{2,3}+\mathscr{A}_{1,2}\mathscr{B}_{2,3}+\frac{1}{2}\mathscr{C}_{1+2-3,1,2,3}H_{1+2-3}\right.$$
$$\left.+\mathscr{B}_{1,3}\mathscr{B}_{3,2}\left[H_{3-2}H_{3-1}+H_{2-3}H_{1-3}\right]\right\} \quad \text{(A23)}$$

Inspecting the expression for the envelope kurtosis it is seen that κ_4 does not depend on the matrix $\mathscr{D}$ which represents the contribution of third harmonics while both κ_{40} and κ_{04} do depend on $\mathscr{D}$ but with opposite sign so that the envelope kurtosis $\kappa_{40}+2\kappa_{22}+\kappa_{04}$ becomes independent of the third harmonic. For equal variance of η and ζ one may give an even more general argument why the envelope kurtosis is independent of the third harmonics. This is related to Eq. (A18) which shows that the envelope kurtosis depends on $\langle|Z|^4\rangle$ only and it is straightforward to prove that to lowest significant order third harmonics cannot contribute to this fourth moment of Z.

I finally checked the general results for the kurtosis by taking the limit of a narrow-band wave train. Using (A4) one finds

$$\begin{aligned}\kappa_{40} &= 24m_0\left(\gamma+\beta+2(\alpha+\Delta)^2\right),\\ \kappa_{22} &= 8m_0\left(\gamma+\alpha^2+(\alpha+\Delta)^2\right),\\ \kappa_{04} &= 24m_0\left(\gamma-\beta+2\alpha^2\right),\end{aligned} \quad \text{(A24)}$$

so that the envelope kurtosis assumes the form

$$\kappa_4 = 64m_0\left(\gamma+\alpha^2+(\alpha+\Delta)^2\right), \quad \text{(A25)}$$

and exactly the same results for the kurtosis parameters are found when one starts from the single mode representation (A5) following the method in Janssen (2009).

The single mode results give a reasonable approximation to the statistics of the case of a wind sea spectrum. We use these results to illustrate for a significant steepness of $\varepsilon = k_0 m_0^{1/2} = 0.1$ the dependence of the skewness factor C_3 and the kurtosis factor $C_4 = \kappa_4/8$ on dimensionless depth $k_0 h$. This is shown in Fig. 9. Note the sensitive dependence of these statistical factors for a dimensionless depth in the range of 1-2.

A.4 Nonlinear simulations and the exponential distribution.

It is important to validate a number of results obtained in this note by means of a Monte Carlo simulation. Since the interest is in extreme events with probabilities of the order 10^{-6} the number of ensemble members N_{ens} needs to be quite large. By trial and error, I have taken $N_{ens} = 50,000,000$, in order to obtain smooth results for the pdf. A numerical simulation using the complex envelope function given in (A1)-(A3) would therefore be very expensive because it involves 8-dimensional integrations in wavenumber space. However, assuming that the envelope waveheight pdf is determined by the skewness factor C_3 and the kurtosis factor C_4 only, one may use any nonlinear system in the numerical simulation as long as it

has the same statistical parameters. For this reason a Monte Carlo simulation is therefore performed with a single wave train given by Eq. (A5), where the amplitude a is drawn from a Rayleigh distribution while the random phase is drawn from a uniform distribution. Up to a significant steepness of 0.1 (which is very extreme) the formula for the envelope kurtosis (A25) and the skewness (A13) agree in a satisfactory manner with the results from the numerical simulations. We have also studied the properties of the envelope waveheight of this nonlinear system. The envelope waveheight pdf, as obtained from the Monte Carlo Simulation, is shown in Fig. 10. In this example the parameters $\alpha, \beta, \gamma,$ and Δ have been chosen in

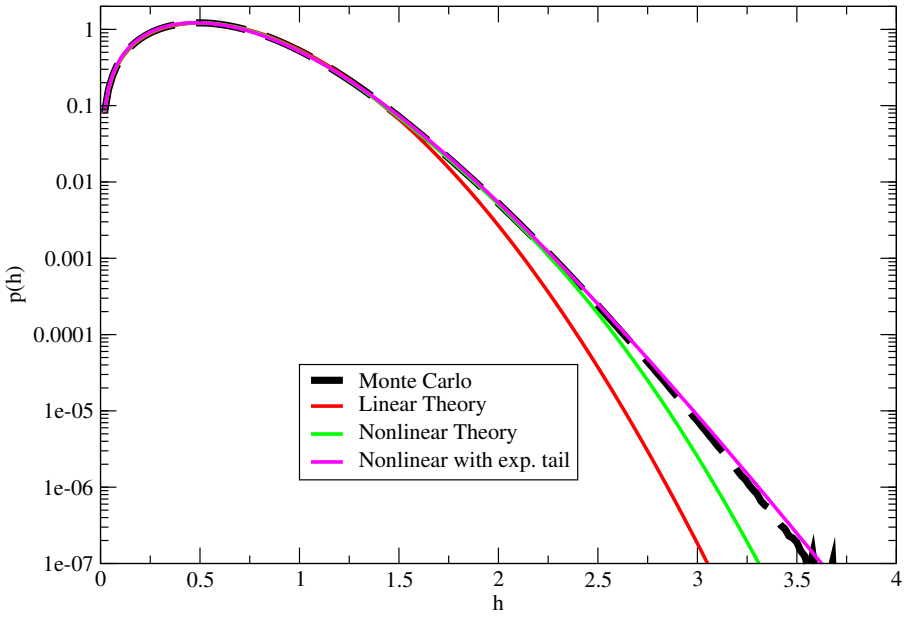

Figure 10: Probability distribution function of envelope wave height for a significant steepness of 0.06 and a dimensionless depth of 1.45, mimicking the Draupner wave event. The Monte Carlo simulation shows clear evidence that the tail of the distribution is exponential. Nonlinear theory combined with the stretched exponential of Residori is in good agreement with the simulation.

such a way that they match the statistical parameters found from the numerical simulation of the sea state when the Draupner wave event occurred. In particular given the skewness factors $C_3 = 0.0678$ and the kurtosis factor $C_4 = 0.0425$ as found during the Draupner event, the parameters α and Δ are determined from (A14) and (A25) with the result

$$\alpha^2 = (C_4 - 2C_3^2)/4m_0, \; \Delta = C_3/2m_0^{1/2} - \alpha,$$

while $\gamma = -\alpha^2/2$ and β is unspecified because the skewness and envelope kurtosis do not depend on the amplitude of third-order harmonics in lowest significant order. I have tried several values for β and as long as the third-harmonic amplitude has a value of order ε^3 the resulting envelope wave height pdf is very similar indeed.

Over a wide range of values, between 10^{-6} and 10^{-2}, the pdf behaves as a straight line, hence the pdf follows an exponential law. For comparison, also shown are results according to linear theory, and it is clear that this gives a large underestimation of the frequency of extreme events. The nonlinear theory discussed by Janssen (2014) shows good agreement with the simulation up to a waveheight of

$h = 2.5$, but the probability of extreme events such as the Draupner case with $h = 3.1$ are considerably underestimated. The approach that adds, using the method detailed in §2.3, a stretched exponential is found to agree very well with the numerical simulation.

References

Adler, R.J., 1981. *The Geometry of Random Fields*, John Wiley, 275 pp.

Benetazzo, A., F. Barbariol, F. Bergamasco, A. Torsello, S. Carniel, and M. Sclavo, 2015. Observation of Extreme Sea Waves in a Space-Time Ensemble. *J. Phys. Oceanogr.* **45**, 2261-2275.

Baxevani, A. and I. Rychlik, 2006. Maxima for Gaussian Seas. *Ocean Eng.* **33**, 895-911

Benjamin, T.B., and J.E. Feir, 1967: The desintegration of wavetrains on deep water. Part 1. Theory. *J. Fluid Mech.* **27**, 417-430.

Cavaleri, L., F. Barbariol, A. Benetazzo, L. Bertotti, J.-R. Bidlot, Peter A.E.M. Janssen and Nils Wedi, 2015. The Draupner wave: a fresh look and the emerging view.

Fedele F., 2012. Space-Time Extremes in Short-Crested Storm Seas. *J. Phys. Oceanogr.* **42**, 1601-1615.

Goda, Y., 2000. *Random seas and Design of Maritime Structures*. 2nd ed. World Scientific, 464 pp.

Janssen, Peter A.E.M., 2003. Nonlinear Four-Wave Interactions and Freak Waves. *J. Phys. Oceanogr.* **33**, 863-884.

Janssen, Peter A.E.M., 2009. On some consequences of the canonical transformation in the Hamiltonian theory of water waves, *J. Fluid Mech.* **637**, 1-44.

Janssen, Peter A.E.M., 2014. On a random time series analysis valid for arbitrary spectral shape, *J. Fluid Mech.* **759**, 236-256.

Janssen, Peter A.E.M., 2015, Notes on the maximum wave height distribution. ECMWF Technical Memorandum 755.

Janssen Peter A.E.M and Miguel Onorato, 2007. The intermediate water depth limit of the Zakharov Equation and consequences for wave prediction, *J. Phys. Oceanogr.* **37**, 2389-2400.

Janssen, Peter A.E.M., and Jean-R. Bidlot, 2009. On the extension of the freak wave warning system and its verification. ECMWF Technical Memorandum 588.

Montina, A., U. Bortolozzo, S. Residori, and F.T. Arecchi, 2009. Non-Gaussian Statistics and Extreme Waves in a Nonlinear Optical Cavity, PRL **103**, 173901.

Mori N. and P.A.E.M. Janssen, 2006. On kurtosis and occurrence probability of freak waves. *J. Phys. Oceanogr.* **36**, 1471-1483.

Stefania Residori, 2015. Private communication and presentation at Cargèse summerschool on Rogue Waves.

Walczak, Pierre, Stéphane Randoux, and Pierre Suret, 2015. Optical Rogue Waves in integrable turbulence. PRL **114**, 143903.

Worsley, K.J., 1996. The geometry of random images. *Chance*, **9**, 27-40.